

BARWISE COMPRESSION SCHEMES FOR AUDIO-BASED MUSIC STRUCTURE ANALYSIS

Axel Marmoret **Frédéric Bimbot**
 Univ Rennes, Inria, CNRS, IRISA, France.
 firstname.name@irisa.fr

Jérémie E. Cohen
 CNRS, CREATIS, Villeurbanne France.
 jeremy.cohen@cnrs.fr

ABSTRACT

Music Structure Analysis (MSA) consists in segmenting a music piece in several distinct sections. We approach MSA within a compression framework, under the hypothesis that the structure is more easily revealed by a simplified representation of the original content of the song.

More specifically, under the hypothesis that MSA is correlated with similarities occurring at the bar scale, linear and non-linear compression schemes can be applied to barwise audio signals. Compressed representations capture the most salient components of the different bars in the song and are then used to infer the song structure using a dynamic programming algorithm.

This work explores both low-rank approximation models such as Principal Component Analysis or Nonnegative Matrix Factorization and “piece-specific” Auto-Encoding Neural Networks, with the objective to learn latent representations specific to a given song. Such approaches do not rely on supervision nor annotations, which are well-known to be tedious to collect and possibly ambiguous in MSA description.

In our experiments, several unsupervised compression schemes achieve a level of performance comparable to that of state-of-the-art supervised methods (for 3s tolerance) on the RWC-Pop dataset, showcasing the importance of the barwise compression processing for MSA.

1. INTRODUCTION

Music Structure Analysis (MSA) consists in subdividing a music piece in several distinct parts, which represent a mid-level description of a song. Segmentation is usually based on criteria such as homogeneity, novelty, repetition and regularity [1].

When performed algorithmically, MSA often relies on similarity criteria within passages of a song summarized in an autosimilarity matrix [2–8], in which each coefficient represents an estimation of the similarity between two musical fragments.

While similarity between two frames can be obtained from the feature representation of the signal, such as the STFT of the song [2], recent works try to design new representations of the original music, able to capture the similarity

between two frames while maintaining a high level of dissimilarity between dissimilar frames [1, 3–8]. This generally consists in projecting the data in a new feature space and computing the similarity in the feature space.

In most former work, the similarity is expressed between beatwise aligned features, as in [4, 5]. Instead, the present work considers that repetitions are more prone to happen at the barscale, and hence focuses on barwise aligned features, as in [7]. A comparison between both has been made in [8], without one singling out.

In this work, we first explore low-rank approximation methods to perform barwise dimensionality reduction using Principal Component Analysis (PCA) and Nonnegative Matrix Factorization (NMF). We also design “piece-specific” Auto-Encoding Neural Networks (AE). While linear dimensionality reduction is a standard method nowadays, the work presented in this article is the first one, as far as we know, to consider barwise dimensionality reduction. Moreover, we extend the concept of barwise compression to the use of a song-dependent autoencoder, *i.e.* an AE which is specifically trained to compress a given song. This technique is called “Single-Song Auto-Encoding” (SSAE) and the latent representation of each bar in the AE is used as a sequence of features for segmenting the song.

Indeed, recently, Deep Neural Networks (DNN) have led to some high level of excitement in Music Information Retrieval (MIR) research, and notably in MSA [9, 10]. In general, DNN approaches rely on large databases which make it possible to learn a large number of parameters, which in turn yields better performance than previously established machine learning approaches. This is the consequence of the ability of DNNs to learn complex nonlinear mappings through which musical objects can be expected to be better separated [11]. Hence, while DNNs generally learn “deep” features stemming from multiple examples in a training phase, and then evaluate the potential of learned features [12], our SSAE approach focuses on the different events within a single song and tries to learn nonlinear latent representations, used to infer the structure.

To study the relevance of the barwise compression approach, this work evaluates different dimensionality reduction techniques on the RWC-Pop dataset [13] in their audio form using various time-frequency features.

The rest of the article is structured as follows: section 2 details the motivations and approaches for barwise music compression, section 3 presents various compression schemes used in this work, section 4 presents the segmentation process, and section 5 reports on the experimental

results.

2. BARWISE MUSIC COMPRESSION

2.1 Motivations

The underlying idea of this work is that music structure can be related to compression of information. Indeed, a common view of music structure is to consider structural segments as internally coherent passages, and automatic retrieval techniques generally focus on finding them by maximizing homogeneity and repetition and/or by setting boundaries between dissimilar segments, as points of high novelty [1].

In the context of compressed representations, each passage is transformed in a vector of small dimension, compelling this representation to summarize the original content. From this angle, similar passages are expected to be represented by similar representations, as they share underlying properties (such as coherence and redundancy), while dissimilar passages are bound to create strong discrepancies at their boundaries. Thus, we expect that compressed representations will enhance the original structure while reducing incidental signal-wise properties which do not constitute to the structure.

Conversely to fixed-size frame analysis, barwise computation guarantees that the information contained in each frame does not depend on the tempo, but on the metrical positions, which is a more abstract musical notion to describe time. As a consequence, comparing bars is more reliable than comparing frames of arbitrarily fixed size as it allows to cope with small variations of tempo.

In addition, pop music (*i.e.* our case study) is generally quite regular at the bar level: repetitions occur at the bar scale and motivic patterns tend to develop within a limited number of bars, suggesting that frontiers mainly sit between bars.

Accordingly, the proposed method relies on a consistent bar division of music. It also requires a powerful tool to detect bars, as otherwise errors could propagate and affect the performance. Results reported in [7] tend to show that the madmom toolbox [14] is efficient in that respect on the RWC-Pop dataset. Nonetheless, this processing may hinder the retrieval of boundaries based on a change of tempo, as discussed in [15]. It also relies on some consistent bar division of music, which is generally the case for contemporary western music, but is not a universal rule, and/or may turn out to be ambiguous.

2.2 Barwise Music Processing

Following our former work in [7], we process music as barwise spectrograms, with a fixed number of frames per bar. Practically, spectrograms are computed using librosa [16] with a low hop length of 32 frames at a sampling rate of 44.1kHz, and downbeats are estimated with the madmom toolbox [14]. This allows us to split the original spectrogram in b barwise spectrograms (b being the number of bars in this song) each containing n_b frames. As bars can be of different lengths (because of tempi differences or small inconsistencies/imperfections in the performance),

different bars can contain different numbers n_b of frames. Thus, we define a subdivision s parameter, which is the desired number of frames in each bar

Starting from the subdivision s , and from indexes f_s and f_e , respectively the indexes of the closest frames to the downbeats starting and ending the bar, we select all frames $\left\{ \frac{f_s + k \times (f_e - f_s)}{s}, 0 \leq k < s \right\}$, *i.e.* equally-spaced frames in the bar to fit the chosen subdivision. This indeed results in barwise spectrograms containing exactly s frames. Other techniques could be applied to reduce the number of frames (for example averaging the content of several frames instead of choosing one), but we did not pursue that lead. We chose $s = 96$ as in [7].

This technique result in b barwise Time-Frequency spectrograms, of size $f \times s$, with f the number of components in the chosen feature, as presented in section 2.3. Compression is generally performed on matrices (as PCA and NMF for instance). In that sense, by vectorizing each of the previous barwise spectrograms, we introduce the “barwise TF” representation, consisting in a matrix of size $b \times fs$. The aformentioned process is described in Figure 1. Note that we chose to vectorize the time-frequency features, thus discarding the dependencies between these two dimensions.

2.3 Features

Music is represented with different features throughout our experiments, focusing on different aspects of music such as harmony or timbre.

Chromagram A chromagram represents the time-frequency aspect of music as sequences of 12-row vectors, corresponding to the 12 semi-tones of the classical western music chromatic scale (C, C#, ..., B), which is largely used in Pop music. Hence, $f = 12$, and each row represents the weight of a semi-tone (and its octave counterparts) at a particular instant.

Mel spectrogram A Mel spectrogram corresponds to the STFT representation of a song, whose frequency bins are recast in the Mel scale. These bands account for the exponential spread of frequencies throughout the octaves. Mel spectrograms are dimensioned following the work of [9] (80 filters, from 80Hz to 16kHz), hence $f = 80$. STFT are computed as power spectrograms.

Log Mel spectrogram (LMS) A Log Mel spectrogram (abbreviated “LMS”) corresponds to the logarithmic values of the precedent spectrogram, hence f is still equal to 80. This representation accounts for the exponential decay of power with frequency observed in STFT.

Nonnegative Log Mel spectrogram (NNLMS) Nonnegative Log Mel spectrogram (abbreviated “NNLMS”) is a nonnegative version of the precedent LMS. This representation is motivated by the fact that some compression algorithms are nonnegative (in particular, NMF), and thus need nonnegative inputs. NNLMS are computed as $\log(Mel + 1)$ where Mel represent the coefficients of the Mel spectrogram, and \log the elementwise logarithm. Interestingly, as it will be demonstrated in Section 5.3, compression algorithms generally obtain similar results in both LMS and NNLMS representation.

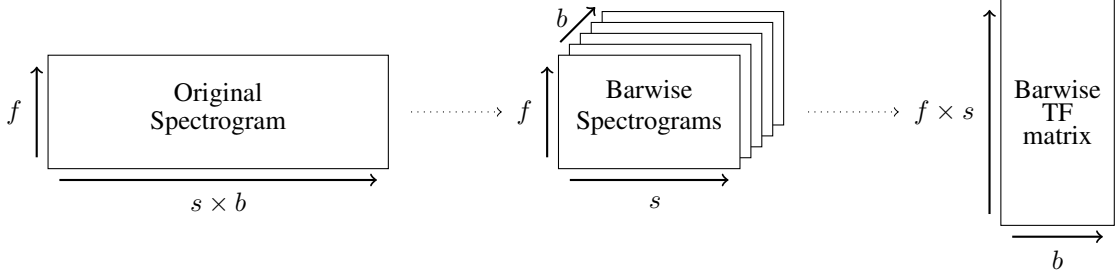


Figure 1: Barwise processing of an input spectrogram, resulting in a barwise TF matrix.

MFCC spectrogram Mel-Frequency Cepstral Coefficients (MFCCs) are timbre-related coefficients, obtained by a discrete cosine transform of a Log Mel spectrogram¹. This spectrogram contains $f = 32$ coefficients, following [17].

3. COMPRESSION SCHEMES

3.1 Low-Rank Approximations

Given a collection of input vectors $\{x_i\}_{i=1,\dots,b} \in \mathbb{R}^n$ stored in a matrix X , low-rank approximations search for projections in a low-dimensional subspace which approximates the input vectors.

PCA is maybe the most well-known and used low-rank approximation technique. It can be seen as a singular value decomposition applied on the debiased matrix $X - \mu$, where μ is the mean of the columns of X . In short, we obtain an approximation $X - \mu \approx WH$ where $W \in \mathbb{R}^{n \times d_c}$ is orthogonal, and $H \in \mathbb{R}^{d_c \times b}$ is the product of a diagonal and an orthogonal matrix. The rank of the approximation d_c is chosen by the user, and should be smaller than both dimensions.

NMF is similar to PCA but does not impose orthogonality, nor does it unbias the data. Instead, it builds a cone containing the data, which extreme rays are the columns of W . To achieve this, nonnegativity is required elementwise on both W and H . The low-rank approximation is in fact the solution of an optimization problem, here $\text{argmin}_{W \geq 0, H \geq 0} \|X - WH\|_F^2$ using the Frobenius norm as a loss function. NMF typically yields more interpretable features than PCA, but it is much harder to compute, and requires that the data is mostly nonnegative [18].

3.2 Autoencoders

Autoencoders are neural networks, which, by design, perform unsupervised dimensionality reduction. Throughout the years, AE have received increasing interest, notably due to their ability to extract salient latent representations without the need of large amount of annotations. Recently, AE also showed great results as a generation tool [19, 20]. Still, as presented in [20], PCA and AE are competitive as compression schemes, and PCA even leads to lower reconstruction error when AE are too “simple” (in particular when networks are linear or “shallow”, *i.e.* with only a few layers).

¹ Note that we use the default librosa settings for MFCC, hence the Log Mel spectrogram used for MFCC is not the same as the LMS presented before.

Practically, given a generic entry $x \in \mathbb{R}^n$, an AE learns a nonlinear function f with parameters θ (weights and biases of the network) such that $\hat{x} = f(x, \theta) \in \mathbb{R}^n$ reconstructs x as faithfully as possible. This is achieved by minimizing a given loss function such as the Mean Square Error (MSE) between x and \hat{x} w.r.t. parameters θ .

$$\arg \min_{\theta} \text{MSE}(x, \hat{x}) = \frac{1}{n} \sum_{i=0}^{n-1} (x_i - \hat{x}_i)^2. \quad (1)$$

Other metrics can be used, such as the KL-divergence, but we restrict this work to MSE.

An autoencoder is divided into two parts: an encoder, which compresses the input $x \in \mathbb{R}^n$ into a latent representation $z \in \mathbb{R}^{d_c}$ of smaller dimension (generally, $d_c \ll n$), and a decoder, which reconstructs \hat{x} from z .

In this work, layers are of two types: fully-connected, or convolutional. Convolutional layers lead to impressive results in image processing due to their ability to discover local correlations (such as lines or edges), which turn to higher-order features with the depth of the network [21] [22, Ch. 9]. While local correlations are less obvious in spectrogram processing [23], Convolutional Neural Networks (CNN) still perform well in MIR tasks, such as MSA [9].

The tested AE is hence a CNN. We use the nowadays quite standard ReLu function as the activation function, except in the latent layer because it could lead to null latent variables. The encoder is composed of five hidden layers: 2 convolutional/max-pooling blocks, followed by a fully-connected layer, controlling the size d_c of the latent space. Convolutional kernels are of size 3x3, and the pooling is of size 2x2. Convolutional layers define respectively 4 and 16 feature maps.

The decoder is composed of 3 hidden layers: a fully-connected layer (inverse of the previous one) and 2 “transposed convolutional” layers of size 3x3 and stride 2x2. A transposed convolution is similar to the convolution operation taken in the backward pass: an operation which takes one scalar as input and returns several scalars as output [24, Ch. 4]. Hence, it is well suited to inverse the convolution process. This network is represented in Figure 2.

3.3 Dimensions of Compression

Selecting the dimension of the compression d_c , *i.e.* the number of components to use for compressing the input data, is not trivial. In particular, it is well-known that selecting the number of components for NMF is a complex

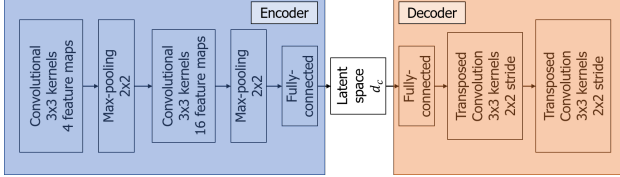


Figure 2: Architecture of the autoencoder

problem, generally leading to manual tuning or dedicated heuristics [18, 25]. We also observed a great influence of the size of the latent space of the AE on the segmentation results, without a clear candidate singling out. In that sense, we will compare values for $d_c \in \{8, 16, 24, 32, 40\}$.

Even if such heuristics are standard for PCA (such as the elbow method), as no obvious candidate heuristic stood out relatively to the quality of segmentation, and for fair comparison with other techniques, PCA will be tested with the same d_c values. A clever dimension selection could be studied in future work.

4. STRUCTURAL SEGMENTATION

4.1 General Principle

The ability of these compression methods to separate and group bars is evaluated on the MSA task, as presented in [26].

Thereby, for a given song in a given representation, we obtain compressed representations z_i for all bars $1 \leq i \leq b$ of the song. These compressed representations are at the heart of the segmentation strategy, via their autosimilarity matrix.

Denoting $Z \in \mathbb{R}^{d_c \times b}$ the matrix resulting from the concatenation of all d_c -dimensional z_i vectors, its autosimilarity is defined as $Z^T Z$, *i.e.* the $b \times b$ matrix of the dot products between every z_i . These dot products are then normalized to 1, resulting in a matrix of cosine similarities. Examples of autosimilarities are shown in Figure 3.

Segmentation is obtained via the dynamic programming algorithm presented in [7], and inspired from [27]. The principle of dynamic programming is to solve a combinatorial optimization problem by dividing it in several atomic problems, easier to solve, and which solutions can be stiched together to form the global solution. The Viterbi and Dynamic Time Warping (DTW) algorithms are examples of dynamic programming algorithms with a lot of applications in the Audio community.

In our context, a “segmentation cost” is computed for every segment in the song. These individual segment costs constitutes the atomic problems to solve. Then, the optimal segmentation consists in the global maximum of the sum of the segment costs for all the segments in this segmentation.

The cost of each segment is designed in order to favor their homogeneity. As the autosimilarity matrix represent the similarity between pairs of bars in the song, the higher is this similarity, the most similar are the bars. Hence, the cost of a segment is defined as an aggregated value of the similarity between all pairs of bars in this segment. Practically, this is obtained by convolving a kernel with the au-

tosimilarity restricted to this segment. Hence, to compute the cost of each segment in the song, the algorithm applies a sliding convolving kernel on the diagonal of the autosimilarity matrix. This convolving kernel is a square matrix, the size of which is that of the potential segment.

While sharing the principle of a sliding kernel with the work of Foote [2], largely described in the literature [1], the proposed kernel focuses on homogeneity rather than novelty. When the diagonal of the autosimilarity is structured in several self-similar blocks, the algorithm frames and partitions these blocks.

4.2 Technical Details

The design of the kernel defines how to transform bar similarities to segment homogeneity in the form of a cost. A kernel matrix full of ones would imply that the segment cost is the sum of the similarity values in this segment. The proposed kernel is equal to 0 on the diagonal, 2 on the lower and upper 4 sub-diagonals, and 1 everywhere else. The diagonal is equal to zero so as to disregard perfect self-similarity of each bar with itself (normalized to 1). The other elements of this kernel are designed so as to emphasize the short-term similarity in the 4 contiguous bars, and still catch longer-term similarity for long segments. This kernel performs best in comparative experiments² of [7], and, notably, better than a kernel matrix of 1 with a 0 diagonal.

To account for regularity constraints as in [27], the present algorithm adds a regularity penalty $p(n)$ to the plain convolution score, which is a function of the size n (in bars) of the segment. This function $p(n)$ is equal to 0 if $n = 8$, $\frac{1}{4}$ if $n = 4$, $\frac{1}{2}$ if $n \equiv 0 \pmod{2}$, and finally 1 otherwise. This penalty function is musically motivated for pop music, as segments are more likely to be of size 4 or 8 bars (especially in RWC-Pop with MIREX10 annotations [27]), than of odd bar size, as shown in Figure 5.

Finally, for all possible segments b_1, b_2 in the song, the algorithm computes a score $s_{b_1, b_2} = \frac{c_{b_1, b_2}}{c_{k8}^{max}} - p(n)$, where c_{b_1, b_2} is the convolution cost, and where c_{k8}^{max} is the highest convolution score on this autosimilarity with a kernel of size 8, used for normalization purposes.

5. EXPERIMENTS

The proposed segmentation pipeline is studied on the RWC-Pop dataset, which consists in 100 Pop songs of high recording quality [13], along with the MIREX10 annotations [28]. We focus on boundary retrieval and ignore segment labelling.

Boundaries are evaluated using the hit-rate metric, which considers a boundary valid if it is approximately equal to an annotation, within a fixed tolerance window. Consistently with MIREX standards [29], tolerances are equal to 0.5s and 3s. The hit-rate is then expressed in terms of

² <https://gitlab.inria.fr/amarmore/musicntd/blob/v0.2.0/Notebooks/5%20-%20Different%20kernels.ipynb>

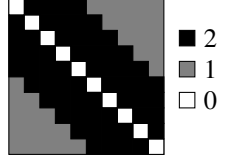


Figure 4: Kernel of size 10

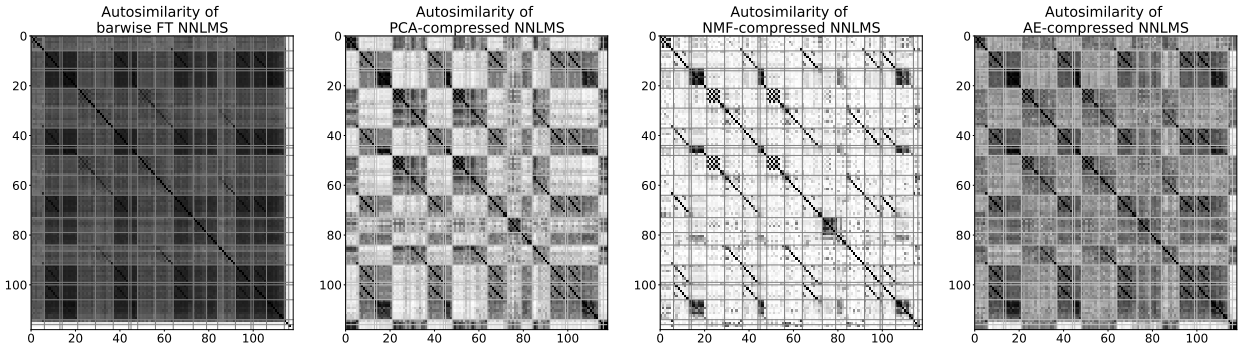


Figure 3: Barwise autosimilarities for the Nonnegative Log Mel spectrogram (left) and of the compressed representation with $d_c = 24$ (from left to right: PCA, NMF and AE) computed on the song “Pop01” from RWC-Pop. Grey lines represent the annotation.

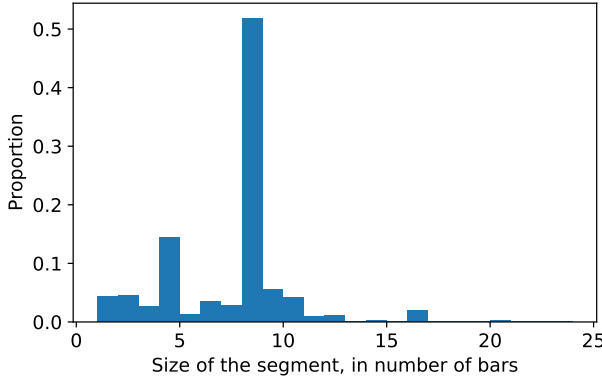


Figure 5: Distribution of segment’ sizes in number of bars in MIREX10.

Precision, Recall, and F-measure, resulting respectively in $P_{0.5}$, $R_{0.5}$, $F_{0.5}$, P_3 , R_3 , F_3 .

5.1 Related Work

Related work mainly splits in two categories: blind and learning-based techniques.

Blind segmentation techniques, such as this work, do not use training datasets and generally focus on autosimilarity matrices. The seminal paper in this area is the work of Foote [2], based on a novelty kernel, which detects boundaries as points of strong dissimilarity between the near past and future of a given instant. The strong point of this algorithm is its good performance given its relative simplicity.

Later on, McFee and Ellis made use of spectral clustering as a segmentation method by interpreting the autosimilarity as a graph and clustering principally connected vertices as segments [4]. This work performed best among blind segmentation techniques in the last structural segmentation MIREX campaign in 2016 [29]. Recently, we used tensor decomposition (Nonnegative Tucker Decomposition, NTD) as a way to describe music as barwise patterns, which then served as features for the computation of an autosimilarity matrix [7].

Still, to the best of the authors’ knowledge, the current state-of-the-art approach for the task of RWC-Pop dataset structural segmentation is a supervised CNN developed by Grill and Schlüter [9]. This technique also uses signal self-

similarity as input, but in the form of lag matrices, and in conjunction with Log Mel spectrograms.

We compared the barwise compression schemes described in the present work with the aforementioned techniques. Results for [2] and [4] were computed with the MSAF toolbox [30], and boundaries were aligned to the closest downbeat for fairer comparison (as in [7]). Results for [9] were taken from the 2015 MIREX campaign [29].

5.2 Practical Considerations

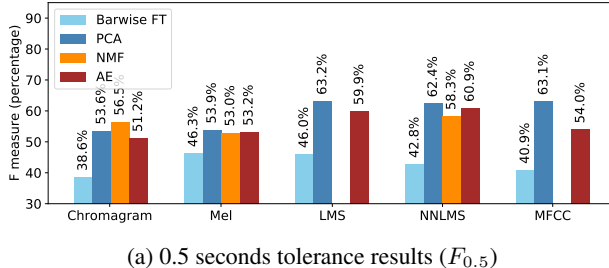
PCA is computed with the scikit-learn [31] toolbox, using the ARPACK solver. NMF is computed using the nn_fac toolbox [32]. The AE is developed with Pytorch 1.8.0 [33], optimized with the Adam optimizer [34], with a learning rate of 0.001, divided by 10 when the loss function reaches a plateau (20 iterations without improvement) until 1e-5. The optimization stops if no progress is made during 100 consecutive epochs, or after a total of 1000 epochs. The network is initialized with the uniform distribution defined in [35], also known as “kaiming” initialization. Bars were estimated with madmom [14], and spectrograms computed with librosa [16] with default settings, unless specified. All segmentation scores were computed with mir_eval [36].

The entire code for this work is open-source, and contains experimental notebooks for reproducibility³. Performing 1000 epochs for a song takes between 1.5 minute (for chromagrams) and 5 minutes (for Mel/Log Mel spectrograms) on an Intel® Core(TM) i7 CPU, NMF takes less than 3 seconds and PCA less than a second.

5.3 Results

Figure 6 presents results on the RWC-Pop dataset for all the methods and the features. The dimension of compression d_c is chosen as the best performing one for the F_3 metric. The Log Mel and Nonnegative Log Mel spectrogram seem to outperform the other features at both tolerances, except for the PCA which obtain similar performances with MFCC. PCA and AE achieve the state-of-the-art level of performance with 3-seconds tolerance, as presented in Table 1. With 0.5-second tolerance, all techniques obtain lower results than those of the state-of-the-

³ <https://gitlab.inria.fr/amarmore/BarwiseMusicCompression>



(a) 0.5 seconds tolerance results ($F_{0.5}$)

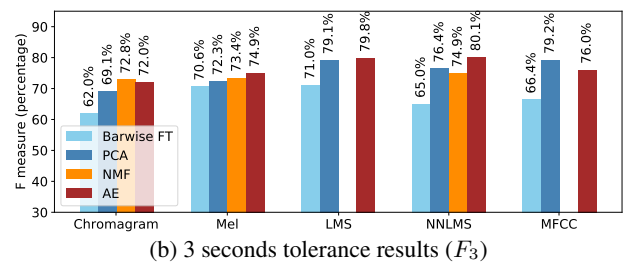


Figure 6: Segmentation results for the different methods and representation.

Table 1: Results of best-performing methods and state-of-the-art on the RWC-Pop dataset. (*Results: 2015 MIREX contest [29].)

		$P_{0.5}$	$R_{0.5}$	$F_{0.5}$	P_3	R_3	F_3
Compression methods	PCA	60.7%	66.9%	63.1%	76.1%	84.0%	79.2%
	NMF	57.4%	60.4%	58.3%	73.6%	77.6%	74.9%
	Autoencoder	60.1%	62.6%	60.9%	78.9%	82.5%	80.1%
State-of-the-art	Foote [2]	42.0%	30.0%	34.5%	67.1%	47.7%	55.0%
	Spectral clustering [4]	49.2%	45.0%	45.0%	65.5%	60.6%	60.3%
	NTD [7]	58.4%	60.7%	59.0%	72.5%	75.3%	73.2%
	Supervised CNN [9]*	80.4%	62.7%	69.7%	91.9%	71.1%	79.3%

art. Still, all methods are competitive with the blind state-of-the-art.

NMF obtain lower results than the other methods, but, due to the nonnegativity, it is expected that NMF result in a part-based decomposition of the original barwise spectrogram. The part-based property can lead to interpretable factors, as observed in many applications [18, 37], and is important for pattern uncovering in NTD [7]. Nonetheless, in this study, we do not have quantitative results to support this claim.

Results are consistent with those of [20], where PCA obtain similar or better reconstruction errors than linear or shallow autoencoders. Still, we believe that the presented AE can be greatly improved.

Finally, results seem still improvable with 0.5-second tolerance. A wrong estimation at 0.5s can be due to an incorrect frontier estimation, but also to an incorrect bar estimation.

6. CONCLUSION

Barwise compression schemes appear as competitive schemes for Music Structure Analysis. In our experiments, the Log Mel and Nonnegative Log Mel features outperform the other ones (except for MFCC with the PCA), and reaches the state-of-the-art at 3-seconds tolerance on the RWC-Pop music dataset.

Future work will focus on improving the proposed paradigm, for instance with nonlinear compression methods such as kernel methods, or by improving the autoencoder in using strategies such as transfer learning from a song-independent AE or exploring various network architectures or regularizations. Finally, while the convolutional dynamic programming algorithm is competitive, it is unstable to small variations in autosimilarities and should be made more robust.

Altogether, we believe that these first results pave the way to an interesting paradigm using barwise compression algorithms, and notably single-song AEs, for the description of structural elements in music.

7. REFERENCES

- [1] O. Nieto, G. J. Mysore, C.-i. Wang, J. B. Smith, J. Schlueter, T. Grill, and B. McFee, “Audio-based music structure analysis: Current trends, open challenges, and applications,” *Trans. Int. Soc. for Music Information Retrieval*, vol. 3, no. 1, 2020.
- [2] J. Foote, “Automatic audio segmentation using a measure of audio novelty,” in *2000 IEEE Int. Conf. Multimedia and Expo. ICME2000. Proc. Latest Advances in the Fast Changing World of Multimedia*, vol. 1. IEEE, 2000, pp. 452–455.
- [3] J. Serra, M. Müller, P. Grosche, and J. L. Arcos, “Unsupervised music structure annotation by time series structure features and segment similarity,” *IEEE Transactions on Multimedia*, vol. 16, no. 5, pp. 1229–1240, 2014.
- [4] B. McFee and D. Ellis, “Analyzing song structure with spectral clustering,” in *Int. Soc. Music Information Retrieval (ISMIR)*, 2014, pp. 405–410.
- [5] O. Nieto and T. Jehan, “Convex non-negative matrix factorization for automatic music structure identification,” in *2013 IEEE Int. Conf. Acoustics, Speech and Signal Processing (ICASSP)*. IEEE, 2013, pp. 236–240.
- [6] I. Theodorakopoulos, G. Economou, and S. Fotopoulos, “Unsupervised music segmentation via multi-scale processing of compressive features’ representation,” in

- 2013 18th International Conference on Digital Signal Processing (DSP). IEEE, 2013, pp. 1–6.
- [7] A. Marmoret, J. Cohen, N. Bertin, and F. Bimbot, “Uncovering audio patterns in music with nonnegative tucker decomposition for structural segmentation,” in *ISMIR*, 2020, pp. 788–794.
- [8] J.-C. Wang, J. B. Smith, W.-T. Lu, and X. Song, “Supervised metric learning for music structure feature,” *arXiv preprint arXiv:2110.09000*, 2021.
- [9] T. Grill and J. Schlueter, “Music boundary detection using neural networks on combined features and two-level annotations,” in *ISMIR*, 2015, pp. 531–537.
- [10] M. McCallum, “Unsupervised learning of deep features for music segmentation,” in *ICASSP*. IEEE, 2019, pp. 346–350.
- [11] E. Humphrey, J. Bello, and Y. LeCun, “Feature learning and deep architectures: New directions for music informatics,” *J. Intelligent Information Systems*, vol. 41, no. 3, pp. 461–481, 2013.
- [12] R. Agrawal and S. Dixon, “Learning frame similarity using siamese networks for audio-to-score alignment,” in *2020 28th European Signal Processing Conference (EUSIPCO)*. IEEE, 2021, pp. 141–145.
- [13] M. Goto, H. Hashiguchi, T. Nishimura, and R. Oka, “RWC Music Database: Popular, Classical and Jazz Music Databases,” in *ISMIR*, vol. 2, 2002, pp. 287–288.
- [14] S. Böck, F. Korzeniowski, J. Schlueter, F. Krebs, and G. Widmer, “madmom: a new Python Audio and Music Signal Processing Library,” in *Proc. 24th ACM Int. Conf. Multimedia*, Amsterdam, The Netherlands, 10 2016, pp. 1174–1178.
- [15] I. Vatolkin, F. Ostermann, and M. Müller, “An evolutionary multi-objective feature selection approach for detecting music segment boundaries of specific types,” in *Proc. Genetic and Evolutionary Computation Conf.*, 2021, pp. 1061–1069.
- [16] B. McFee *et al.*, “librosa/librosa: 0.8.1rc2.” Zenodo, May 2021. [Online]. Available: <https://doi.org/10.5281/zenodo.4792298>
- [17] B. McFee and D. Ellis, “Learning to segment songs with ordinal linear discriminant analysis,” in *ICASSP*. IEEE, 2014, pp. 5197–5201.
- [18] N. Gillis, *Nonnegative Matrix Factorization*. Philadelphia, PA: Society for Industrial and Applied Mathematics, 2020.
- [19] J. Engel *et al.*, “Neural audio synthesis of musical notes with wavenet autoencoders,” in *Int. Conf. Machine Learning*. PMLR, 2017, pp. 1068–1077.
- [20] F. Roche, T. Hueber, S. Limier, and L. Girin, “Autoencoders for music sound modeling: a comparison of linear, shallow, deep, recurrent and variational models,” *arXiv preprint arXiv:1806.04096*, 2018.
- [21] Y. LeCun, L. Bottou, Y. Bengio, and P. Haffner, “Gradient-based learning applied to document recognition,” *Proc. of the IEEE*, vol. 86, no. 11, pp. 2278–2324, 1998.
- [22] I. Goodfellow, Y. Bengio, and A. Courville, *Deep Learning*. MIT Press, 2016, <http://www.deeplearningbook.org>.
- [23] G. Peeters and G. Richard, “Deep Learning for Audio and Music,” in *Multi-faceted Deep Learning: Models and Data*. Springer, 2021. [Online]. Available: <https://hal.telecom-paris.fr/hal-03153938>
- [24] V. Dumoulin and F. Visin, “A guide to convolution arithmetic for deep learning,” *arXiv preprint arXiv:1603.07285*, 2016.
- [25] B. T. Nebgen, R. Vangara, M. A. Hombrados-Herrera, S. Kuksova, and B. S. Alexandrov, “A neural network for determination of latent dimensionality in non-negative matrix factorization,” *Machine Learning: Science and Technology*, vol. 2, no. 2, p. 025012, 2021.
- [26] J. Paulus, M. Müller, and A. Klapuri, “Audio-based music structure analysis.” in *ISMIR*. Utrecht, 2010, pp. 625–636.
- [27] G. Sargent, F. Bimbot, and E. Vincent, “Estimating the structural segmentation of popular music pieces under regularity constraints,” *IEEE/ACM Trans. Audio, Speech, and Language Processing*, vol. 25, no. 2, pp. 344–358, 2016.
- [28] F. Bimbot, G. Sargent, E. Deruty, C. Guichaoua, and E. Vincent, “Semiotic description of music structure: An introduction to the quaero/metiss structural annotations,” in *53rd Int. Conf. Audio Engineering Soc.*, 2014.
- [29] “MIREX wiki,” https://www.music-ir.org/mirex/wiki/MIREX_HOME.
- [30] O. Nieto and J. Bello, “Systematic exploration of computational music structure research.” in *ISMIR*, 2016, pp. 547–553.
- [31] F. Pedregosa *et al.*, “Scikit-learn: Machine learning in Python,” *Journal of Machine Learning Research*, vol. 12, pp. 2825–2830, 2011.
- [32] A. Marmoret and J. Cohen, “nn_fac: Nonnegative factorization techniques toolbox,” 2020.
- [33] A. Paszke *et al.*, “Pytorch: An imperative style, high-performance deep learning library,” in *Advances in Neural Information Processing Systems 32*. Curran Associates, Inc., 2019, pp. 8024–8035. [Online]. Available: <http://papers.neurips.cc/paper/9015-pytorch-an-imperative-style-high-performance-deep-learning.pdf>

- [34] D. Kingma and J. Ba, “Adam: A method for stochastic optimization,” *arXiv preprint arXiv:1412.6980*, 2014.
- [35] K. He, X. Zhang, S. Ren, and J. Sun, “Delving deep into rectifiers: Surpassing human-level performance on imagenet classification,” in *Proc. IEEE Int. Conf. Computer Vision*, 2015, pp. 1026–1034.
- [36] C. Raffel *et al.*, “mir_eval: A transparent implementation of common MIR metrics,” in *ISMIR*, 2014.
- [37] D. Lee and H. Seung, “Learning the parts of objects by non-negative matrix factorization,” *Nature*, vol. 401, no. 6755, pp. 788–791, 1999.